A phogrin–aequorin chimaera to image free Ca^{2+} in the vicinity of secretory granules

Aristea E. POULI*, Nedim KARAGENC*, Christina WASMEIER†, John C. HUTTON†, Nick BRIGHT‡, Sue ARDEN‡, J. George SCHOFIELD* and Guy A. RUTTER*[1]

*Department of Biochemistry, School of Medical Sciences, University Walk, University of Bristol, Bristol BS8 1TD, U.K., †Barbara Davis Center for Childhood Diabetes, University of Colorado Health Services Center, Box B140, 4200, East, 9th Avenue, Denver, CO 80262, U.S.A., and ‡Department of Clinical Biochemistry, University of Cambridge, Cambridge CB2 2QR, U.K.

Microdomains of high Ca^{2+} concentration ($[Ca^{2+}]$) may be critical to the control of intracellular processes such as secretion and metabolism without compromising other cell functions. To explore changes in $[Ca^{2+}]$ in the outer mantle (< 30 nm deep) that surrounds the surface of dense-core secretory granules, we have designed a recombinant chimaera between the granule protein phogrin and aequorin. When expressed in populations of insulin-secreting MIN6 or phaeochromocytoma PC12 cells, the chimaera was targeted to secretory granules as expected. The recombinant protein reported a similar $[Ca^{2+}]$ at the granule surface to that in the bulk cytosol, measured with untargeted aequorin. This was the case both at rest ($[Ca^{2+}] = 80$–120 nM) and after stimulation with agents that provoke Ca^{2+} entry or Ca^{2+} mobilization from intracellular pools, and during activated secretion. Thus depolarization of MIN6 cell populations with high K^+ increased $[Ca^{2+}]$ both in the bulk cytosol and close to the granules to approx. 4 μM, with near-identical kinetics of increase and recovery. Similarly, stimulation of PC12 cells with ATP provoked an increase in $[Ca^{2+}]$ in either domain to 1.3 μM. These data argue that, in MIN6 and PC12 neuroendocrine cells (i) significant mobilization of Ca^{2+} from most secretory granules probably does not occur during activated Ca^{2+} influx or mobilization of internal Ca^{2+} stores, and (ii) agonist-stimulated Ca^{2+}-dependent secretion can occur without development of a large gradient of $[Ca^{2+}]$ between the surface of most secretory vesicles and the rest of the cytosol.

INTRODUCTION

High local concentrations of Ca^{2+} in the vicinity of dense-core secretory granules are implicated in the stimulation of exocytosis in neuroendocrine and other cells displaying regulated secretion [1]. For example, those granules that are part of or close to a docking complex are likely to experience high local $[Ca^{2+}]$ beneath the plasma membrane [2] resulting from influx of external Ca^{2+}. The resulting elevated Ca^{2+} concentrations may be essential to activate key regulatory proteins of the secretory machinery and to trigger the fusion event [3].

It has also been suggested that granules deeper within the cell may also experience Ca^{2+} levels exceeding those in the bulk cytosol. For example, in acinar cells, Ca^{2+} may be mobilized from the granule itself by the second messengers inositol 1,4,5-trisphosphate (IP_3) or cyclic ADP-ribose [4]. Given the slow diffusion characteristics of Ca^{2+} in the cell cytosol [5], it may be predicted that release of Ca^{2+} from granule stores may produce a domain of high Ca^{2+} around each granule. This could contribute to the fusion of docked granules, and possibly to the transmission of Ca^{2+} waves across the cell by Ca^{2+}-induced Ca^{2+} release.

In order to measure $[Ca^{2+}]$ in the vicinity of the external face of secretory granules ($[Ca^{2+}]_{dg}$) we have fused cDNA encoding the Ca^{2+}-sensitive photoprotein, aequorin, in-frame at the cytosolic C-terminus of a membrane-spanning granule protein, phogrin [6]. Phogrin (112 kDa; 1004 amino acids) was identified in a systematic search for genes encoding proteins localized exclusively on the membrane of secretory granules [6]. Fusion of the protein with aequorin should therefore allow $[Ca^{2+}]$ to be measured specifically in a mantle 10–30 nm from the surface of the granule membrane, i.e. in a domain that would be inaccessible by light microscopy. Using a similar strategy, Marsault et al. [2] have already observed persistently elevated levels of Ca^{2+} beneath the plasma membrane of a smooth-muscle cell line (A7r5).

We have expressed the recombinant phogrin–aequorin chimaera in insulin-secreting MIN6 and adrenal phaechromocytoma PC12 cells and analysed $[Ca^{2+}]$ near the granule membrane and in the bulk cytosol at rest and during activated secretion. When analysed in MIN6 cell populations, stimulation of Ca^{2+} influx after plasma-membrane depolarization by high K^+ provoked increases in $[Ca^{2+}]$ in the domain of the secretory granule, which were closely similar in amplitude and kinetics of onset and relaxation to those of cytosolic Ca^{2+} ($[Ca^{2+}]_c$). However, more sustained increases in $[Ca^{2+}]_{gd}$ were observed in a small subpopulation of single MIN6 cells analysed by photon-counting digital imaging [7]. Stimulation of PC12 cells with ATP provoked changes in $[Ca^{2+}]_c$ and $[Ca^{2+}]_{gd}$ that were very similar. These data imply that the generation of locally high $[Ca^{2+}]$ as a result of Ca^{2+} release from granules, if it occurs at all, plays a very limited role in the activation of secretion in neuroendocrine cells.

MATERIALS AND METHODS

Materials

Fura 2 acetoxymethyl ester, FM1-43 and coelenterazine were obtained from Molecular Probes (Eugene, OR, U.S.A.), and Transfectam™ and Tfx-50™ from Promega. All other reagents were obtained from Sigma (Poole, Dorset, U.K.) or BDH (Poole, Dorset, U.K.). Tissue culture reagents were obtained from Gibco (Paisley, Scotland).

Abbreviations used: IP_3, inositol 1,4,5-trisphosphate; $[Ca^{2+}]_c$ and $[Ca^{2+}]_{gd}$, the concentrations of free ionized Ca^{2+} in the bulk cytosol and the vicinity of the granule membrane, respectively; HA, haemagglutinin; PTP, phosphotyrosine protein phosphatase; KRB, Krebs–Ringer bicarbonate.

[1] To whom correspondence should be addressed.

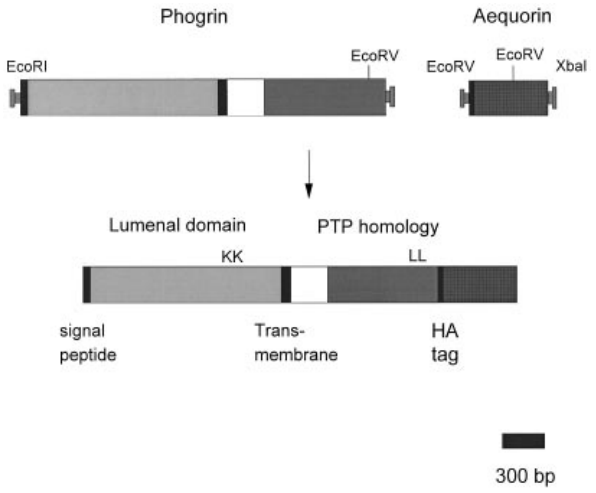

Figure 1 Construction of pCMV.phog.Aq and predicted structure of translated product

cDNA encoding phogrin in plasmic pcDNA3 was fused with an HA–tag–aequorin cDNA generated by PCR, as described in the Materials and methods section. The predicted structure of the translated product is shown, including potential dibasic cleavage site (KK), the dileucine (LL) motif and the phosphoprotein tyrosine phosphatase (PTP) homology domain.

Plasmid construction

cDNA encoding a fusion between the haemagglutinin (HA) epitope tag and apoaequorin [8] was amplified by PCR from vector pCDNA1 using the following primers: primer 1, 5′-TTTTGATATCTATGATGTTCCTGATTAT-3′ (*Eco*RV site underlined) primer 2, 5′-TTTTTCTAGATTAGGGGACAGCTCCACCGTA (*Xba*I site underlined). To avoid cleavage of the internal *Eco*RV site within the aequorin gene-coding region [9], the 618 bp *Eco*RV–*Xba*I fragment was subcloned into the intermediate vector pGEM-T (Promega) and released by partial digestion with *Xba*I and *Eco*RV. cDNA encoding the entire coding region of phogrin within the eukaryotic expression vector pcDNA3 (Invitrogen) was cleaved with *Eco*RV and *Xba*I, and the HA–aequorin fragment inserted to generate plasmid pCMV.phog.Aq (Figure 1). cDNA encoding non-targeted (cytosolic) aequorin [8], subcloned in vector VR1012 (Vical, San Diego, CA, U.S.A.; plasmid pCMV*Aq_c), was kindly provided by Dr. R. Rizzuto (University of Padova, Padova, Italy). Plasmid DNA was purified on CsCl gradients before transfection [10].

Cell culture and transfection

MIN6 cells were cultured in Dulbecco's modified Eagle's medium (Gibco) supplemented with 15% (v/v) foetal bovine serum, 2 mM L-glutamine, 100 U/ml penicillin and 100 μg/ml streptomycin at 37 °C at 5% CO_2. PC12 cells were cultured in Dulbecco's modified Eagle's medium supplemented with 10% (v/v) foetal bovine serum, 5% horse serum, 100 U/ml penicillin and 100 μg/ml streptomycin. Cell lines at 50–60% confluency on glass coverslips were transfected with plasmids (2.5 μg per 22 mm-diameter coverslip, 0.6 μg for 13 mm coverslip), using Tfx-50 (3:1 with respect to DNA) for MIN6 cells or Transfectam™ (2:1 with respect to DNA) for PC12 cells. All transfections were carried out with serum-free medium as described by the manufacturer. Cells were cultured for 48 h at 37 °C and 5% CO_2 before [Ca^{2+}] measurement and imaging.

Immunocytochemistry and immunoelectron microscopy

For immunocytochemistry, transfected cells were fixed with 3% paraformaldehyde and probed with the anti-HA monoclonal 12CA6 (Boehringer-Mannheim, Mannheim, Germany) and revealed with FITC-conjugated anti-mouse IgG secondary antibody. Fluorescence was examined by laser-scanning confocal microscopy using a Leica DMIRBI microscope fitted with a 63×1.4 NA, PL FLUOTAR oil immersion objective. Immunoelectron microscopy of ultrathin sections was performed as described previously [11].

Detection of aequorin luminescence and calculation of [Ca^{2+}]

Cell populations

Transfected cells cultured on 13 mm glass coverslips were washed twice in serum-free medium, and were incubated for a further 90 min in serum-free medium plus 7.5 μM coelenterazine, the prosthetic group of aequorin. This allowed reconstitution of the active aequorin–coelenterazine holoenzyme. Measurements were performed at 37 °C in modified Krebs–Ringer bicarbonate comprising 130 mM NaCl, 3.6 mM KCl, 0.5 mM NaH_2PO_4, 0.5 mM $MgSO_4$, 10 mM NaHepes, 2.0 mM $NaHCO_3$, 1.5 mM $CaCl_2$, and 5.5 mM glucose, equilibrated with O_2/CO_2 (95:5, v/v) (KRB), in a photomultiplier detection system as described [12]. Calibration of [Ca^{2+}] was performed as described previously [12].

Single-cell photon-counting imaging

This was performed at 37 °C essentially as described [7] but using an intensified charge-coupled device camera comprising a low-noise S-20 multi-alkali photocathode and three in-series microchannel plates (Photek ICCD216; Photek Ltd., East Sussex, St. Leonards-on-Sea, Sussex, U.K.). The camera intensifier was maintained at 4 °C and attached to the lower port of an Olympus IX-70 microscope with a UPlanApo 10×0.4 NA air objective. Single-photon events were captured at video rate as a data stream, and held in the buffer of an on-board video card ('Time-resolved imaging'). Images were generated off-line from this stored matrix with the desired integration interval. Other details are given in the Figure legends.

Simultaneous measurement of FM1-43 and fura 2 fluorescence

PC12 cells cultured as described above were loaded sequentially at 25 °C in KRB (see above) with 2 μM fura 2 acetoxymethyl ester (40 min followed by 10 min in the absence of dye to allow ester cleavage) and then 2 μM FM1-43 [(*N*-(3-trimethylammoniopropyl)-4-(*p*-dibutylaminostyryl)pyridinium dibromide; 10 min]. Cells were perifused with KRB supplemented with 2 μM FM1-43 on the thermostatically controlled (37 °C) stage of a Nikon Diaphot inverted microscope, fitted with a 40×1.3 NA for Fluor oil immersion objective. Imaging was performed with a system capable of exciting and detecting four wavelength pairs simultaneously (within 2 s; Improvision, Coventry, U.K.). For fura 2 imaging, cells were excited at 340 and 380 nm. Emitted light was filtered at 455 nm with a dichroic mirror and collected by a single microchannel plate intensified charge-coupled device camera (Photonic Science, Robertsbridge, Sussex, U.K.). For FM1-43 imaging, the excitatory wavelength was 510 nm, and emitted light was again filtered with the dichroic mirror at 455 nm. Video signals were digitized and stored with image-processing software hosted by a Macintosh 8100/100

computer. Background images at each wavelength were acquired from a field lacking cells and subtracted before the calculation of ratio images (fura 2). No autofluorescence was observed at the camera gains used. The 340/380 ratio of fura 2 fluorescence is presented as a semiquantitative estimate of intracellular free [Ca^{2+}].

Other methods

Kinetic analysis was performed using FigP (BioSoft, Cambridge, U.K.). Images were processed where necessary using Adobe Photoshop™ 3.0 (Adobe Systems Inc.) and Freelance-for-Windows™ (Lotus). Statistical analysis was performed using Excel™ (Microsoft), and data are given as means ± S.E.M.

RESULTS

Construction of phogrin–aequorin

The phogrin–aequorin construct used in these studies in shown schematically in Figure 1. The construct encodes the complete phogrin sequence, in which 42 amino acids at the C-terminus have been replaced with an HA epitope tag, plus aequorin. This truncation interrupts the PTP domain, but leaves likely localization sites including a dileucine motif (residues 912 and 913) intact. Transient expression of the construct produced the punctate extranuclear pattern characteristic of granules in both MIN6 and PC12 cells (Figures 2a and 2b). Exclusive granule localization was confirmed in MIN6 cells by immunoelectron microscopy, using a monoclonal antibody against the HA epitope tag of the phogrin–aequorin chimaera (12CA6) and anti-insulin serum (Figure 2c).

Comparison of granule-domain and cytosolic [Ca^{2+}] in MIN6 cell populations

MIN6 cells, a highly differentiated model of parental islet β-cells, possess abundant secretory granules [13] (and see Figure 2c). Further, these cells possessed a pool of Ca^{2+} within an acidic compartment which could be mobilized by treatment with ionomycin and monensin (results not shown). This is likely to represent a store of Ca^{2+} within secretory granules. We examined changes in $[Ca^{2+}]_c$ and $[Ca^{2+}]_{gd}$ in populations of MIN6 stimulated with either ATP (a Ca^{2+}-mobilizing agonist in this cell type; results not shown) or high K^+ (to depolarize the plasma membrane and allow Ca^{2+} influx through voltage-gated Ca^{2+} channels). Both of these manoeuvres provoke cytosolic [Ca^{2+}] increases sufficient to stimulate insulin secretion from the β-cell type [14]. Comparison of the aequorin luminescence signals obtained under these conditions revealed the following (Figure 3): (i) similar or identical basal levels of $[Ca^{2+}]_{gd}$ and $[Ca^{2+}]_c$ (80–120 nM) before stimulation; (ii) a similar rate of increase in [Ca^{2+}] in both domains after stimulation with either ATP or K^+; (iii) similar or identical peak [Ca^{2+}] after K^+ depolarization; (iv) near-identical rates of recovery of $[Ca^{2+}]_c$ and $[Ca^{2+}]_{gd}$ after K^+ depolarization (apparent first-order rate constants, $k_{-1} = 0.0445 \pm 0.0006$ and $0.0456 \pm 0.0007\ s^{-1}$ for $[Ca^{2+}]_c$ and $[Ca^{2+}]_{gd}$ respectively).

Imaging $[Ca^{2+}]_c$ and $[Ca^{2+}]_{gd}$ in single MIN6 cells

We next aimed to confirm that the similar behaviour observed for [Ca^{2+}] in the bulk cytosol and in the granule domain, apparent in cell populations, was also apparent at the level of single cells. This was considered important given the strong dependence of aequorin luminescence on [Ca^{2+}], which can mean that abnormally high [Ca^{2+}] in one or a few cells could heavily bias the mean calibrated value [7]. Using photon-counting digital imaging [7] and an integration period of 10 s, we detected transient changes in $[Ca^{2+}]_c$ after K^+ stimulation [15] in three single MIN6 cells expressing untargeted (cytosolic) aequorin and eight single cells expressing granule-targeted (phogrin) aequorin. Calibration of the peak [Ca^{2+}] values was performed [7] in the cells giving either the greatest or smallest apparent [Ca^{2+}] change from each group. Values of 7 and 21 μM were obtained for two individual cells expressing cytosolic aequorin, and 9.5 and 22 μM for cells expressing phogrin–aequorin. Although somewhat higher than the values predicted from the population traces, probably as a result of threshold phenomena [7], these single-cell values lend strong support to the conclusion that there were no large differences between cytosolic and granule-domain [Ca^{2+}] during plasma-membrane depolarization with K^+.

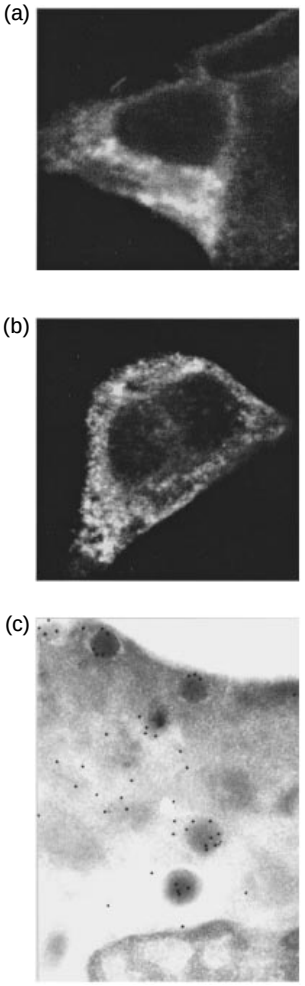

Figure 2 Localization of the phogrin–aequorin chimaera to secretory granules

Single MIN6 (**a**) or PC12 (**b**) cells were transfected with pCMV.phog.Aq, fixed and permeabilized and probed with anti-HA–tag antibody, as described in the Materials and methods section. Note the characteristic punctate fluorescence pattern of secretory granules. (**c**) Immunoelectron microscopy image of an MIN6 cell transfected with pCMV.phog.Aq and probed with antibodies to insulin (10 nm immunogold particles) and HA–tag (5 nm particles). Note the presence of anti-HA immunoreactivity exclusively on the membrane of secretory granules, consistent with the localization of the phogrin–aequorin climaera to this site.

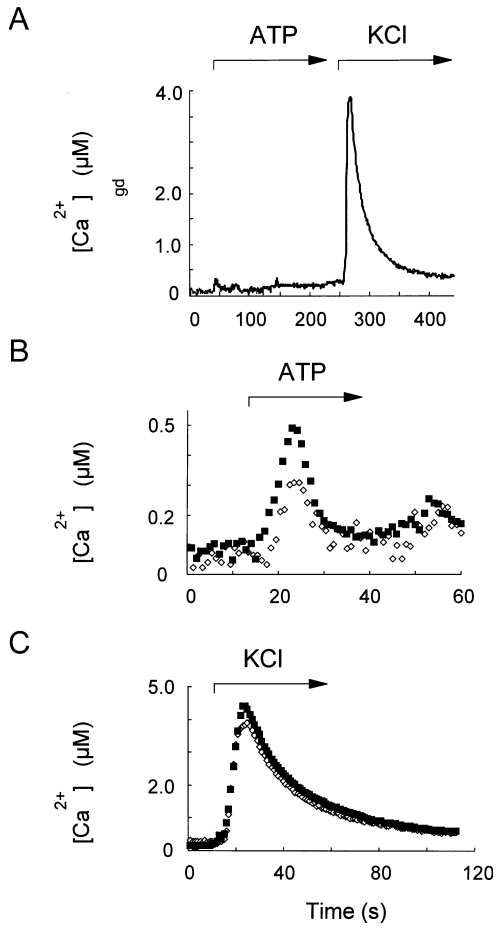

Figure 3 Effect of ATP and high K^+ on $[Ca^{2+}]_c$ and $[Ca^{2+}]_{gd}$ in MIN6 cell populations

Cell populations were transfected with plasmid pCMV*.Aq_c or pCMV.phog.Aq to measure changes in $[Ca^{2+}]$ in either the granule domain (open symbols) or the bulk cytosol (closed symbols). Cells were perifused at 1.0 ml/min with KRB buffer (see the Materials and methods section), and the perifusion medium switched to one containing ATP (100 μM) or KCl (30 mM) as indicated $[Ca^{2+}]$ values were calculated as described in the Materials and methods section. Changes in $[Ca^{2+}]_{gd}$ after sequential stimulation with ATP and KCl are shown in (**A**); identical experiments were performed with untargeted (cytosolic) aequorin to provide a comparison of changes in $[Ca^{2+}]_{gd}$ and $[Ca^{2+}]_c$ after stimulation of cells with ATP (**B**) or with KCl (**C**).

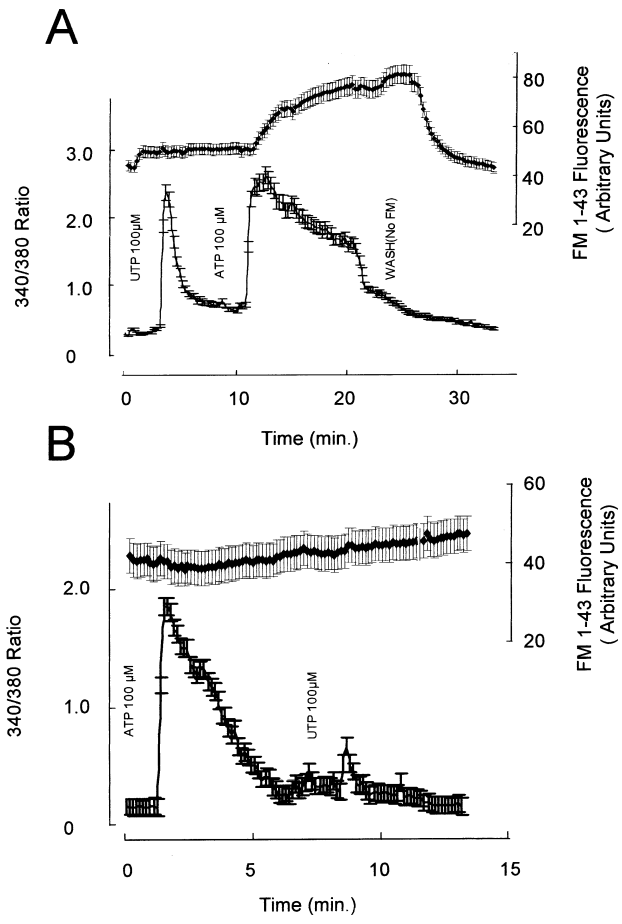

Figure 4 Effects of UTP and ATP on $[Ca^{2+}]$ and exocytotic activity

Fura 2- and FM1-43-loaded PC12 cells were exposed to 100 μM UTP and 100 μM ATP as shown, either in complete KRB medium (Materials and methods section) (**A**) or medium lacking added $CaCl_2$ and supplemented with 1 mM EGTA (**B**). Intracellular $[Ca^{2+}]$ was estimated using the fura 2 fluorescence ratio as shown, and the increase in the total surface area of the plasma membrane estimated by changes in total cellular FM1-43 fluorescence, as described in the Materials and methods section. The data are means $\pm$ S.E.M. of changes observed in eight (**A**) or six (**B**) single cells.

Comparison of granule-domain and cytosolic $[Ca^{2+}]$ in PC12 cell populations

To determine whether there may be differences in $[Ca^{2+}]_{gd}$ and $[Ca^{2+}]_c$ during activated exocytosis in another neuroendocrine cell type, we examined these parameters in phaeochromocytoma PC12 cells [16]. These cells are known to give brisk secretory responses (releasing catecholamines and ATP) on increases in intracellular $[Ca^{2+}]$ [17]. These secretory responses are generally greater than seen with the insulin-secreting MIN6 cells and suggested that single-cell measurements using the lipophilic fluorescent dye FM1-43 [18] may be possible with this cell type; such measurements were not successful with MIN6 cells (results not shown). We first defined conditions providing robust Ca^{2+} dependent secretion in single PC12 cells using FM1-43 and simultaneous imaging of $[Ca^{2+}]_c$ and secretion [18]. FM1-43 is non-fluorescent in aqueous solutions but becomes fluorescent when incorporated into the plasma membrane. Increases in the plasma-membrane area during secretion therefore produce enhanced fluorescence from this fluorophore. Changes in cytosolic $[Ca^{2+}]_c$, measured with fura 2, and in FM1-43 fluorescence were monitored simultaneously in groups of single PC12 cells (Figure 4). These cells responded to challenge with either UTP or ATP with an increase in $[Ca^{2+}]_c$, which was more sustained after ATP stimulation (Figure 4A). However, only ATP provoked a marked and time-dependent increase in FM1-43 fluorescence, compatible with the activation of exocytosis as a result of Ca^{2+} influx (Figure 4A). To confirm that the ATP-stimulated increase in FM1-43 fluorescence reported Ca^{2+}-influx-dependent exocytosis, we stimulated cells with ATP in the absence of extracellular Ca^{2+} (Figure 4B). Whereas intracellular $[Ca^{2+}]$ increases were still observed under these conditions, the apparent secretory response to ATP was completely abolished in the absence of external Ca^{2+} ions. These data are consistent with the behaviour of other PC12 clones [17], and suggest that ATP may provoke exocytosis via the activation of P_{2y}, but not P_{2u}, subtypes of purinergic receptor [19] in these cells.

When changes in granule-domain *versus* bulk cytosolic $[Ca^{2+}]$ were examined in PC12 under conditions where robust Ca^{2+}-

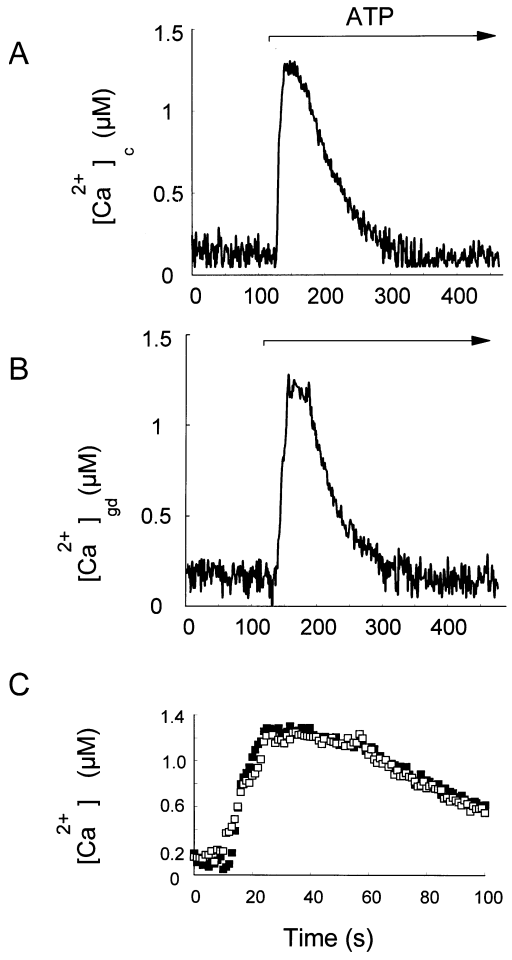

Figure 5 Changes in $[Ca^{2+}]_c$ and $[Ca^{2+}]_{gd}$ in populations of PC12 cells

Cells were transfected with pCMV*Aq_c (**A** or **C**, closed symbols) or pCMV.phog.Aq (**B** or **C**, open symbols) and challenged with 100μM ATP as shown. Note the close identity of the basal and peak [Ca^{2+}] values and the kinetics of changes in the two parameters (bottom panel).

influx-dependent secretion was observed, i.e. stimulation with ATP in the presence of external Ca^{2+}, there were no detectable differences between the kinetics of the [Ca^{2+}] response at the surface of granules and in the bulk cytosol (Figure 5).

We attempted to image changes in $[Ca^{2+}]_c$ and $[Ca^{2+}]_{gd}$ in single aequorin-expressing PC12 cells during ATP stimulation. However, no detectable luminescence response to ATP challenge was apparent, even after hyperexpression of either aequorin construct after direct intranuclear microinjection of plasmic DNA [7] (results not shown). However, this observation can be explained by the fact that the peak [Ca^{2+}] values ($< 1.4\ \mu$M; see Figure 5) did not exceed those required for detection at the single-cell level (see the Discussion and [7]).

DISCUSSION

Measuring [Ca^{2+}] in the granule domain

The fusion of aequorin with a protein uniquely expressed in a single cellular subdomain provides a convenient means of measuring [Ca^{2+}] in that limited subdomain [20]. Although methods of targeting fluorescent probes to intracellular membranes are becoming feasible [21], the ability to use the cell's own sorting machinery to target a reporter molecule provides much more precise targeting to the location desired. From the dimensions of the exposed extragranular domain of phogrin (434 amino acids preceding aequorin), we estimate that the three Ca^{2+}-binding sites of aequorin lie some 5–30 nm from the surface of the granule's lipid bilayer. This estimate is based on the crystallographic dimensions of several proteins, including myosin S1 head [22] (19 nm long; 95 kDa). This is necessarily an approximate estimate given (i) that the high-resolution structure of neither the cytosolic 'tail' of phogrin nor aequorin have been solved; however, the PTP domain of phogrin may be predicted to possess a similar relatively compact structure to that of other members of this family [23]; (ii) the possible flexibility of the chimaeric protein both at its point of exit from the granule membrane and at the phogrin–aequorin junction. Nevertheless, it is possible with the phogrin–aequorin chimaera to measure [Ca^{2+}] in a domain where optical measurements using fluorescent probes and confocal or evanescence wave microscopy [24] (resolution no better than 100–200 nm) are inadequate.

Using this technique, we present the first direct analysis of [Ca^{2+}] in the region of cytosol that surrounds dense-core secretory vesicles. In this way we have been able to compare $[Ca^{2+}]_c$ and $[Ca^{2+}]_{gd}$ dynamically in living cells under a variety of circumstances (active secretion, Ca^{2+} mobilization and Ca^{2+} influx). When combined with photon-counting digital imaging, the recombinant aequorin probe can also give an estimate of $[Ca^{2+}]_{gd}$ within a single cell (although imaging [Ca^{2+}] around a single granule is not feasible at present). In our previous studies applying photon-counting digital imaging to monitor [Ca^{2+}] with recombinant aequorin in small mammalian cells [7], we were unable to detect changes in the cytosolic compartment, whereas those within mitochondria were readily measurable. This was because changes in $[Ca^{2+}]_c$ fell below the threshold of detection. In the current studies, the protocol used to depolarize MIN6 cells with high K^+ provoked a sufficiently large rise in $[Ca^{2+}]_c$ that this could now be measured at the single-cell level. In this way, we have been able to compare changes in $[Ca^{2+}]_c$ with those in $[Ca^{2+}]_{gd}$ within individual cells.

Role of granule Ca^{2+} mobilization in secretion

Our data indicate that, under almost all conditions, the gradient of [Ca^{2+}] between the mantle surrounding granules and the rest of the cytosol is small or non-existent for the bulk of the granule population. Thus, most secretory granules appear never to experience the very high Ca^{2+} concentrations (up to 100 μM) [2] that may exist immediately beneath the plasma membrane of stimulated cells. Whether granules docked for exocytosis to indeed experience these Ca^{2+} concentrations cannot, however, be confirmed by the present technique. However, during the recovery of [Ca^{2+}] to basal levels after stimulation of Ca^{2+} influx into MIN6 cells, [Ca^{2+}] in the granule domain may decay slightly less rapidly than in the bulk cytosol in some individual cells (Figures 3B and 3C). This phenomenon may reflect elevated [Ca^{2+}] sensed by granules in close apposition to the plasma membrane, and therefore to elevated [Ca^{2+}] resulting from stimulated Ca^{2+} influx through voltage-sensitive (L-type) Ca^{2+} channels. By contrasts, $[Ca^{2+}]_{gd}$ values observed after stimulation of MIN6 populations with ATP (Figure 3B) were consistently lower than the corresponding $[Ca^{2+}]_c$ values. This observation perhaps suggests that, in this cell type, secretory granules are partially 'shielded' from the release of Ca^{2+} from internal stores, existing in a microdomain in which [Ca^{2+}] values never achieve those of the bulk cytosol.

The absence of large differences between $[Ca^{2+}]_{gd}$ and $[Ca^{2+}]_c$ in stimulated MIN6 cells, and in PC12 cells undergoing active

secretion, appears to indicate that either (i) Ca^{2+} is not mobilized from granules under these conditions or (ii) any mobilization from granules is unable to generate a gradient of $[Ca^{2+}]$ (high close to the release site). Of these possibilities, option (i) may be the most reasonable, given the known limited diffusional characteristics of Ca^{2+} [25] and the ability to detect persistent gradients of Ca^{2+} using aequorin targeted to the inner surface of the plasma membrane with a SNAP25–aequorin fusion protein [2]. Consistent with this view, data in acinar cells pointing to the presence of IP_3 and cyclic ADP-ribose receptors on dense-core granules [4] have recently been questioned in studies using highly purified granule preparations [26]. Similarly, immunocytochemical evidence that implicated the presence of IP_3 receptors on the dense-core granule membrane of insulin-secreting RINm5F cells [27] has been seriously criticized [28]. Indeed, our data appear to be more supportive of earlier studies [29,30], which indicated that Ca^{2+} could not be mobilized from isolated secretory granules by IP_3 or other agents. Instead, granule Ca^{2+} stores may represent an inert pool of these ions [31], rather than a dynamic one as suggested by early radioisotope exchange studies [32]. Nevertheless, our current data do not absolutely exclude the possibility that Ca^{2+} released from granules is rapidly cleared by adjacent endoplasmic-reticulum, plasma-membrane or mitochondrial Ca^{2+} pump/uptake systems. However, even if such a specialized 'channelling' system between granules and these other stores does exist, it would seem remarkable that differences between $[Ca^{2+}]$ in the granule domain and the rest of the cytosol are not more apparent.

Work in the authors' laboratories was supported by the Wellcome Trust, The Medical Research Council (U.K.), the British Diabetic Association, The Royal Society and the Juvenile Diabetes Foundation. We thank Dr. Rosario Rizzuto (University of Padova) for helpful discussion.

REFERENCES

1 Tse, F. W., Tse, A., Hille, B., Horstmann, H. and Almers, W. (1997) Neuron **18**, 121–132
2 Marsault, R., Murgia, M., Pozzan, T. and Rizzuto, R. (1997) EMBO J. **16**, 1575–1581
3 Rothman, J. E. (1994) Nature (London) **372**, 55–63
4 Gerasimenko, O. V., Gerasimenko, J. V., Belan, P. V. and Petersen, O. H. (1996) Cell **84**, 473–480
5 Clapham, D. E. (1995) Cell **80**, 259–268
6 Wasmeier, C. and Hutton, J. C. (1996) J. Biol. Chem. **271**, 18161–18170
7 Rutter, G. A., Burnett, P., Rizzuto, R., Brini, M., Murgia, M., Pozzan, T., Tavare, J. M. and Denton, R. M. (1996) Proc. Natl. Acad. Sci. U.S.A. **93**, 5489–5494
8 Brini, M., Marsault, R., Bastianutto, C., Alverez, J., Pozzan, T. and Rizzuto, R. (1995) J. Biol. Chem. **270**, 9896–9903
9 Inouye, S., Noguchi, M., Sakaki, Y., Takagi, Y., Toshiyuki, M., Iwanaga, S., Miyata, T. and Tsuji, F. I. (1985) Proc. Natl. Acad. Sci. U.S.A. **82**, 3154–3158
10 Sambrook, J., Fritsch, E. F. and Maniatis, T. (1989) Molecular Cloning: a Laboratory Manual, Cold Spring Harbor Laboratory Press, Cold Spring Harbor, NY
11 Ponnambalam, S., Rabouille, C., Luzio, J. P., Nilsson, T. and Warren, G. (1994) J. Cell Biol. **125**, 253–259
12 Rutter, G. A., Theler, J., Murta, M., Wollheim, C. B., Pozzan, T. and Rizzuto, R. (1993) J. Biol. Chem. **268**, 22385–22390
13 Miyazaki, J., Araki, K., Yamato, E., Ikegami, H., Asano, T., Shibasaki, Y., Oka, Y. and Yamamura, K. (1990) Endocrinology **127**, 126–132
14 Wollheim, C. B. and Sharp, G. W. (1981) Physiol. Rev. **6**, 914–973
15 Theler, J., Mollard, P., Geúrineau, N., Vacher, P., Pralong, W., Schlegel, W. and Wollheim, C. B. (1992) J. Biol. Chem. **267**, 18110–18117
16 Pozzan, T., Gatti, G., Dozio, N., Vicentini, L. M. and Meldolesi, J. (1984) J. Cell Biol. **99**, 628–638
17 Barry, V. A. and Cheek, T. R. (1994) J. Cell Sci. **107**, 451–462
18 Smith, C. B. and Betz, W. J. (1996) Nature (London) **380**, 531–534
19 Nikodijevic, B., Sei, Y., Shin, Y. and Daly, J. W. (1994) Cell. Mol. Neurobiol. **14**, 27–47
20 Rizzuto, R., Brini, M., Bastianutto, C., Marsault, R. and Pozzan, T. (1995) Methods Enzymol. **260**, 417–428
21 Horne, J. H. and Meyer, T. (1997) Science **276**, 1690–1693
22 Rayment, I., Rypniewski, W. R., SchmidtBase, K., Smith, R., Tomchick, D. R., Benning, M. M., Winkelmann, D. A., Wesenberg, G. and Holden, H. M. (1993) Science **261**, 50–58
23 Su, X. D., Taddei, N., Stefani, M., Ramponi, G. and Nordlund, P. (1994) Nature (London) **370**, 575–578
24 Steyer, J. A., Horstmann, H. and Almers, W. (1997) Nature (London) **388**, 474–478
25 Clapham, D. (1995) Cell **80**, 259–268
26 Yule, D. I., Ernst, S. A., Ohnishi, H. and Wojcikiewiez, R. J. H. (1997) J. Biol. Chem. **272**, 9093–9098
27 Blondel, O., Moody, M. M., Depaoli, A. M., Sharp, A. H., Ross, C. A., Swift, H. and Bell, G. I. (1994) Proc. Natl. Acad. Sci. U.S.A. **91**, 7777–7781
28 Meldolesi, J. and Pozzan, T. (1995) Trends Neurosci. **18**, 340–341
29 Prentki, M., Janjic, D. and Wollheim, C. B. (1984) J. Biol. Chem. **259**, 14054–14058
30 Rhodes, C. J., Dawson, A. P. and Hutton, J. C. (1989) in Methodological Developments in Biochemistry (Reid, E., ed.), pp. 281–288, Longman, London
31 Hutton, J. C., Penn, E. J. and Peshavaria, M. (1983) Biochem. J. **210**, 297–305
32 Abrahamsson, H., Gylfe, E. and Hellman, B. (1981) J. Physiol. (London) **311**, 541–550

Received 22 September 1997/27 November 1997; accepted 16 December 1997